LASER–PLASMA INTERACTION DIAGNOSTICS FOR ICF FUSION RESEARCH

W. Seka,[a] R. S. Craxton,[a] R. L. Keck,[a] J. P. Knauer,[a] D. D. Meyerhofer,[a] S. P. Regan,[a] C. Stoeckl,[a] B. Yaakobi,[a] R. E. Bahr,[a] D. Montgomery,[b] H. Baldis,[c] R. Kirkwood[d]

1. INTRODUCTION

Understanding of the coupling of laser light to the plasma corona is essential for the success of laser-driven inertial confinement fusion (ICF). The most desirable way of imparting laser energy to the target plasma is via inverse bremsstrahlung absorption.[1] In addition, at elevated intensities, the thresholds for various instabilities may be exceeded, channeling laser energy into scattered electromagnetic (EM) waves and various electrostatic waves. As a result, part of the incident laser energy may be unavailable for heating the plasma and the target may be irradiated less uniformly. Furthermore, some of the laser energy may ultimately be transferred to energetic electrons that can preheat the fuel and degrade target performance. Many of these processes, such as stimulated Brillouin scattering (SBS), stimulated Raman scattering (SRS), two-plasmon-decay (TPD) instability, and filamentation, have been studied extensively.[2] Presently, however, the understanding of these processes is not sufficient to predict their importance under realistic ICF plasma conditions. Therefore continued surveying of laser–plasma interaction processes is required to guard against unforeseen surprises. This paper surveys the plasma diagnostics used on the OMEGA laser facility at the University of Rochester's Laboratory for Laser Energetics (LLE).

[a]Laboratory for Laser Energetics, University of Rochester, Rochester, NY 14623.
[b]Los Alamos National Laboratory, Los Alamos, NM.
[c]ILSA, Lawrence Livermore National Laboratory and Dept. of Appl. Sciences, University of California at Davis, CA.
[d]Lawrence Livermore National Laboratory, Livermore, CA.

Advanced Diagnostics for Magnetic and Inertial Fusion, Edited by Stott *et al.*
Kluwer Academic/Plenum Publishers, New York, 2002

2. PLASMA DIAGNOSTICS AND RESULTS

Absorption measurements on OMEGA are obtained from 17 plasma calorimeters placed inside the target chamber that consist of dual, thin (25-μm) Ta foils attached to low-mass thermocouples. A Cu pad with equally low thermal mass serves as reference. One of the Ta foils is covered with a UV-transmitting window that measures the scattered UV energy, while the second foil is open and measures the total energy of the scattered UV light, plasma, and x rays. The plasma plus x-ray energy is obtained by subtracting the UV signal from the open-foil signal. The calorimeters are absolutely calibrated using particle beams and UV sources. The random error is ~5%, and the systematic error is estimated at ~4%. For plastic-shell OMEGA implosion experiments, the absorption fractions range between 70% and 80%, depending on the target and pulse shape used. The measurements generally agree with the predictions from hydrodynamic code simulations.

Parametric interaction processes generally do not impart useful energy to the imploding target. Depending on the process, the drive energy may be reduced, the irradiation uniformity may be decreased, or the fuel may be preheated by energetic electrons. A detailed survey of interaction processes on OMEGA is obtained by monitoring the light scattered back through the focusing lens of two of OMEGA's 60 beams. A schematic layout of the full aperture backscatter stations (FABS) is shown in Fig. 1. A 4% pickoff reflection is focused by a near-normal-incidence concave mirror. A 351-nm high reflector separates the UV and visible energies, which are then measured by two volume-absorbing calorimeters. The UV (SBS) calorimeter is cross-calibrated and the visible calorimeter (SRS) is absolutely calibrated and corrected for all intervening optical components. The estimated error on the energy measurements is 5% to 10%

Another two 4% reflections are used to image the target onto two large-core (435-μm) gradient-index fibers filtered for 351 nm (SBS) and the visible for SRS. The two fibers are routed to two spectrometers, each coupled to a streak camera for time-resolved spectroscopy. Typical SBS and SRS spectra are shown in Fig. 2. The broadband SRS spectra have been corrected for group-velocity dispersion in the fiber. Modal dispersion in the fiber is insignificant. The overall time resolution is 80 ps for SBS and 100 ps for SRS. The corresponding spectral resolutions are 0.04 nm (SBS) and 4 nm (SRS).

Figure 3 shows the results obtained from the two FABS's on OMEGA for SBS when two different beam-smoothing techniques are employed, i.e., 2-D SSD[3] at 1-THz

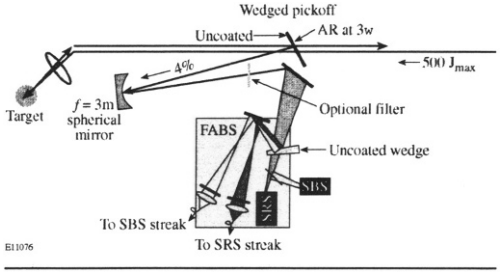

Figure 1. Schematic layout of the full-aperture backscatter station (FABS) on OMEGA, which measures the energy and temporal evolution of the spectrum in the SBS- and SRS-wavelength regions.

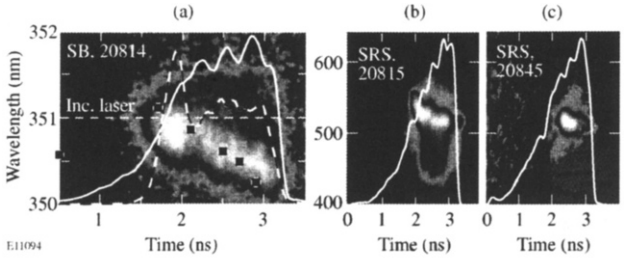

Figure 2. Typical time-resolved SBS (a) and SRS [(b) (c)] spectra obtained on OMEGA long-scale-length interaction experiments at 1-THz SSD beam smoothing. The short-wavelength (at $\lambda \lesssim 500$ nm) SRS emission (b) originates in filaments. Application of polarization smoothing suppresses filamentation and the short-wavelength SRS signal (c). Laser pulse shapes are superposed on all spectra. In (a) the dashed line is the spectrally integrated SBS backscattered power; the squares represent calculated SBS shifts using 2-D hydrodynamic predictions and SBS threshold calculations.

bandwidth with and without polarization smoothing. The two sets of data are clearly separated (○ and ■). Replotting the data for polarization smoothing at half their nominal peak intensity collapses the two sets of data to a single set (● and ■), which leads to the conclusion that SBS primarily originates in the highest-intensity speckles of the intensity distribution.

Parametric interaction processes involving plasma waves are likely to generate energetic electrons.[1] Plasma waves generated by SRS typically give rise to hot-electron temperatures of T_h = 40 to 60 keV, while the TPD plasma waves lead to T_h = 50 and 150 keV. These hot electrons generate x-rays, which are measured with filtered photomultiplier-scintillator detectors.[4] The absolute energy contained in the hot electrons is obtained via cross-calibration using absolutely calibrated x-ray spectroscopy.[5] For ICF studies, the scaling of the temperature and energy content in the fast electrons is important for assessing their possible detrimental impact on target performance. An example of the scaling of T_h with overlapped irradiation intensity is shown in Fig. 4. These data indicate that the TPD instability is susceptible to multibeam-interaction effects contrary to conventional wisdom.

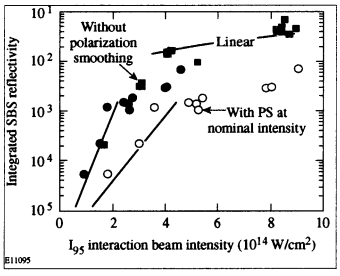

Figure 3. SBS reflectivities obtained in single-beam, long-scale-length, laser–plasma interaction experiments on OMEGA with 1-THz SSD beam smoothing, with (○) and without (■) PS. The ● are data with PS plotted at half their nominal intensities.

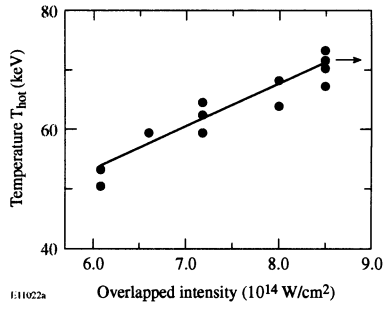

Figure 4. Scaling of hot-electron temperature with overlapped beam intensity inferred from time-resolved, hard-x-ray measurements in the range from 50 to 500 keV. The data were taken with filtered photomultiplier-scintillator detectors on 60-beam OMEGA implosion experiments.

Filamentation in the underdense corona affects the uniformity of target irradiation by expelling plasma from the high-intensity speckles in the light distribution. This process has a low threshold that increases with laser bandwidth when SSD is applied. Filamentation is difficult to measure directly, but there are indirect indicators for it, such as the short-wavelength SRS signal[6] at $\lambda \lesssim 500$ nm (for $\lambda_{\text{Laser}} = 351$ m). Interaction experiments on OMEGA have shown clear evidence for suppression of filamentation in experiments with 1-THz SSD [Figs. 2(b) and (c)].

The temperature T_e influences the instability thresholds and gains. Thus, knowing T_e helps to interpret of interaction experiments.[7] In planar-target experiments T_e has been measured using small (~0.1 μm thick and 200 μm in diam) embedded micro-dots of KCl, Ti, or V. The hydrodynamics of the overall plasma are not measurably influenced by the presence of these dots. Time-resolved x-ray spectroscopy then yields electron temperatures from time-varying x-ray line ratios.

3. CONCLUSION

A wide array of plasma diagnostics supports the interaction experiments on the 60-beam OMEGA laser facility. The results obtained from these experiments continue to refine our understanding of the interaction processes and lead to improved target designs for future large laser fusion facilities (NIF in the US and LMJ in France).

4. ACKNOWLEDGEMENT

This work was supported by the U.S. Department of Energy Office of Inertial Confinement Fusion under Cooperative Agreement No. DE-FC03-92SF19460, the University of Rochester, and the New York State Energy Research and Development Authority. The support of DOE does not constitute an endorsement by DOE of the views expressed in this article.

5. REFERENCES

1. W. L. Kruer, *The Physics of Laser–Plasma Interactions, Frontiers in Physics*, Vol. 73, edited by D. Pines (Addison-Wesley, Redwood City, CA, 1988), Chap. 4, pp. 37–43.
2. H. A. Baldis, E. M. Campbell, and W. L. Kruer, Laser plasma interactions, in: *Handbook of Plasma Physics*, edited by A. Rubenchik and S. Witkowski, Physics of Laser Plasma, edited by M. N. Rosenbluth and R. Z. Sagdeev (North-Holland, Amsterdam, 1991), Vol. 3, pp. 361–434.
3. S. Skupsky, R. W. Short, T. Kessler, R. S. Craxton, S. Letzring, and J. M. Soures, Improved laser-beam uniformity using the angular dispersion of frequency-modulated light, *J. Appl. Phys.* **66**(8), 3456–3462 (1989).
4. C. Stoeckl, V. Yu. Glebov, D. D. Meyerhofer, W. Seka, B. Yaakobi, R. P. J. Town, and J. D. Zuegel, Hard x-ray detectors for OMEGA and NIF, *Rev. Sci. Instrum.* **72**(1), 1197–1200 (2001).
5. B. Yaakobi, C. Stoeckl, T. Boehly, D. D. Meyerhofer, and W. Seka, Measurement of preheat due to fast electrons in laser implosions, *Phys. Plasmas* **7**(9), 3714–3720 (2000).
6. R. W. Short and A. Simon, Collisionless damping of localized plasma waves in laser-produced plasmas and application to stimulated raman scattering in filaments, *Phys. Plasmas* **5**(12), 4134–4143 (1998).
7. S. P. Regan, D. K. Bradley, A. V. Chirokikh, R. S. Craxton, D. D. Meyerhofer, W. Seka, R. W. Short, A. Simon, R. P. J. Town, B. Yaakobi, J. J. Caroll III, and R. P. Drake, Laser-plasma interactions in long-scale-length plasmas under direct-drive national ignition facility conditions, *Phys. Plasmas* **6**(5), 2072–2080 (1999).